Accepted Manuscript

Superlattice in austenitic Ni-Mn-Ga shape memory microwires

Zhiyi Ding, Qingli Qi, Dan Wu, Junpeng Liu, Xiaoming Sun, Yimin Cui, Ming Yue, Yong Zhang, Jie Zhu

PII: S0925-8388(18)34052-0

DOI: https://doi.org/10.1016/j.jallcom.2018.10.353

Reference: JALCOM 48171

To appear in: *Journal of Alloys and Compounds*

Received Date: 31 July 2018

Revised Date: 26 October 2018

Accepted Date: 27 October 2018

Please cite this article as: Z. Ding, Q. Qi, D. Wu, J. Liu, X. Sun, Y. Cui, M. Yue, Y. Zhang, J. Zhu, Superlattice in austenitic Ni-Mn-Ga shape memory microwires, *Journal of Alloys and Compounds* (2018), doi: https://doi.org/10.1016/j.jallcom.2018.10.353.

Superlattice in austenitic Ni-Mn-Ga shape memory microwires

Zhiyi Ding[a], Qingli Qi[a], Dan Wu[b], Junpeng Liu[c], Xiaoming Sun[a], Yimin Cui[a], Ming Yue[b], Yong Zhang[a], Jie Zhu[a,]*

[a] *State Key Laboratory for Advanced Metals and Materials, University of Science and Technology Beijing, 30 Xueyuan Rd., Beijing 100083, People's Republic of China*

[b] *College of Materials Science & Engineering, Beijing University of Technology, Beijing, People's Republic of China*

[c] *State Key Laboratory of Nonlinear Mechanics, Institute of Mechanics, Chinese Academy of Sciences, Beijing 100190, China*

***Corresponding author**: Jie Zhu, Ph.D., Professor*

E-mail: jiezhu@ustb.edu.cn, dingery@163.com

ABSTRACT

The link between microstructure evolution, micromodulated domain and the structure transformation of Ni-Mn-Ga shape memory microwires prepared with rapid solidification is studied systematically by TEM and HRTEM. Multiple microdomain structures are determined according to the corresponding diffraction spots. The domain structure with a periodic distortion is a kind of characteristic of premartensitic phase. When cooling below the martensitic transformation temperature, the austenitic phase transforms to modulated 5M martensite, and the sequence of phase transformation can finally be confirmed from austenite to premartensite to 5M martensite during cooling. The characterization of micromodulated domain and the structure characteristics of austenite at atomic scale provide comprehensive understanding on the martensitic phase transformation route.

Keywords: Shape memory alloys, Premartensitic phase, Micromodulated domain structure, Martensitic transformation

1. Introduction

The first order solid-state martensitic phase transition in ferromagnetic shape memory alloys (FSMAs) gives rise to multi-functional properties, such as superelasticity, shape memory effect and elastocaloric effect [1-5]. Among the FSMAs, stoichiometric Ni_2MnGa Heusler alloy and its derivatives Ni-Mn-X (In, Sn, Sb) in shape memory alloys (SMAs) systems have attracted great attention recently [6-12]. Martensitic transformation consists of a lattice distortion when evolving from the parent phase with $L2_1$ structure to the martensitic phases which include tetragonal five-layered, orthorhombic seven-layered and tetragonal non-layered crystallography lattices in Ni-Mn-Ga system [13]. Premartensitic (PM) transformation, which is usually considered as the appearance of a precursor state, is a kind of weak first-order transition. The origin of modulation or shuffling is related to a TA_2 soft acoustic phonon mode of the austenitic phase at a wave vector q~1/3, which is corresponding to a minimum on the slowest transversal phonon branch and it is associated with nesting features of the Fermi surface [14, 15]. Meanwhile, several kinds of abnormal properties on elasticity [16], thermology [17], electricity [18] and magnetism are found during phase transformation [19-22]. The driving role of the electronic structure and its relationship with the lattice dynamics have been indicated by first-principle calculation [14] and experimental measurements on SMAs [23]. Various kinds of structural transformation characteristics have also been reported in Cu-Zn-Al [24], Ni-Ti [25, 26], Ni-Fe-Ga [27], Eu_2In [28] phase transition materials and novel high-carbon steels with cubic martensitic structures [29]. PM usually occurs during martensitic transformation from highly symmetric cubic phase (austenite) to lowly symmetric phase (martensite), and this process can be driven by external stimuli such as temperature, magnetic field and applied stress. The PM phase structure of Ni_2MnGa possess the same symmetry of $L2_1$ parent phase [30] and it transforms to martensitic phase through a first order phase transition with a discontinuous change in the unit cell volume as also the modulation wave vector and considerable thermal hysteresis [31, 32]. PM phase is also considered as the intermediate state that plays an important role in linking the structure transformation and the origin of ferromagnetism [30]. There is a discussion on whether this modulation is commensurate [15] or incommensurate [30, 31] although the fact of symmetry breaking during phase transformation.

Ni-Mn-Ga is a multiferroic SMA with ordered paramagnetic and ferromagnetic phase near the phase transformation temperature [31, 33]. The large magnetic field-induced strain (MFIS) (10%) obtained under an applied magnetic field originates from the strong magnetoelastic coupling effect activate twin boundary motion [34]. Meanwhile, large MFIS is closely related to the existence of a long period modulated structure. Here, in order to overcome the intrinsic brittleness of Ni-Mn-Ga SMAs, the Taylor-Ulitovsky method was used to fabricate oligocrystalline structured microwires [35-37]. The rapid solidification process that caused by quenching the melt alloys may lead to a rich variety of microstructures and properties, which has already been observed before [38, 39]. The origin of micromodulated domain structure of PM, magnetoelastic coupling effect, phase transformation and their relationships are required further investigation for Ni-Mn-Ga rapidly solidified alloys. Understanding the characteristics of the PM phase and modulation domain structure is critical to obtain advanced multifunctional properties through martensitic phase transformation. In this work, TEM methods are employed to study the micromodulated structure evolution and phase structural transformation route of Ni-Mn-Ga microwires at various temperatures.

2. Experiment details

The ingots with nominal composition of $Ni_{50}Mn_{30}Ga_{20}$ (at.%) alloy were prepared from high pure elements (>99.9%) using an electric-arc induction furnace and were re-melted four times to ensure homogeneities. The microwires with the diameter of 30-300 μm were fabricated by Taylor-Ulitovsky method, which involved rapid quenching from the melt master alloy. The details of microwire fabrication process were described elsewhere [39, 40]. The chemical composition was determined by a scanning electron microscope (SEM, Zeiss Auriga) equipped with an energy dispersive X-ray spectrometer (EDX), using 20 kV accelerating voltage, 10 mm work distance and >60 s data acquisition time duration. The microstructure analysis at microscope scale was carried out by transmission electron microscopy (TEM, Tecnai F30) and high-resolution transmission electron microscopy (HRTEM). Since the micron scale microwires are too small to fabricate by using electrolysis double spray, ion milling technique is selected. Ion-milling with precision ion polishing system (PIPS, Gatan) were performed to fabricate the samples, which can avoid extra stress that may affect the martensitic transformation.

3. Results and discussion

The prepared Ni-Mn-Ga shape memory microwire is on austenitic phase state (marked as P) with the lattice parameter, a = 5.83 Å, which is the same microwire used in ref [39]. The martensitic phase transformation temperature in the vicinity of room temperature (RT) with the martensitic transition starting temperature (M_s), finishing temperature (M_f) during cooling and the austenitic starting temperature (A_s), finishing temperature (A_f) during heating are 264 K, 261 K and 269 K, 274 K, respectively. The Curie temperature estimated from DSC curve is ~372 K. The average chemical composition of the microwire is confirmed to be $Ni_{52.8}Mn_{23.8}Ga_{23.4}$ (±0.5%, at.%) from the surface and fracture by EDX. The chemical composition deviation from the nominal composition is mainly due to the volatilization of manganese in the preparation of microwires.

Fig.1 shows TEM observation of austenitic phase in Ni-Mn-Ga microwires at RT. The dislocations and the characteristics of labyrinth domain can be seen from the bright field image in Fig. 1(a). Fig.1 (a2), (b1), (c1) and (d1) are the selected area electron diffraction (SAED) pattern obtained at different crystal zone axis. Here, the most obvious feature of the SAED is the satellites, which are surrounding the main diffraction spots. In order to throw light on those characteristics, dark-field micrographs are taken from the selected satellites as shown in (b2) from (b1), (c2) from (c1) and (d2) from (d1), respectively. The dark field image of (b2) and (c2) are obtained from three satellites surrounding various main diffraction spots at <110> and <100> crystal zone axis and they exhibit complex domain structure. Those satellites obtained from the SAED patterns with different configurations under different crystal zone axis. Fig.1 (a3), (b3), (c3), and (d3) are the schematic illumination of the configuration of satellites. High-order diffraction spots also appeared except the main diffraction spots and the surrounding satellites, as shown in (b1) and (c1). The dark field images, such as (b2), (c2) and (d2), exhibited significantly difference compared with the tweed structure i.e., diffuse striation lying along the various axis directions. These kinds of features will be discussed combined with HRTEM results later. Various domain characteristics were also reported to be observed in the as-prepared samples at RT, such as FeSiB [41] microwires, Ni-Fe-Ga [27, 42] systems.

The microstructure characteristics presented in the TEM results could be related to the preparation process of Ni-Mn-Ga microwires. The as-prepared $Ni_{50}Mn_{30}Ga_{20}$ microwires, prepared by rapid solidification from molten liquid metal to microwires with water cooling via the Taylor method, may possess high dislocation density, stacking fault and low atomic degree of order. Meanwhile, the phase transformation temperature of the microwires is very close to RT. Usually, the alloy with the same composition presents martensitic state [43]. For the as-prepared Ni-Mn-Ga microwire, appropriate annealing treatment improves atomic order degree of alloy as well as phase transformation temperature (usually more than ten Kelvins) [44, 45]. It is well-known that the defects such as dislocation and stacking fault are actually beneficial to the martensitic transformation (MT) and they may act as nucleation site for MT. By using ordering annealing, the constituent phase of samples may transform from as-prepared austenite to annealed martensite. In this experiment, the ordered phase was observed from the as-prepared Ni-Mn-Ga microwires.

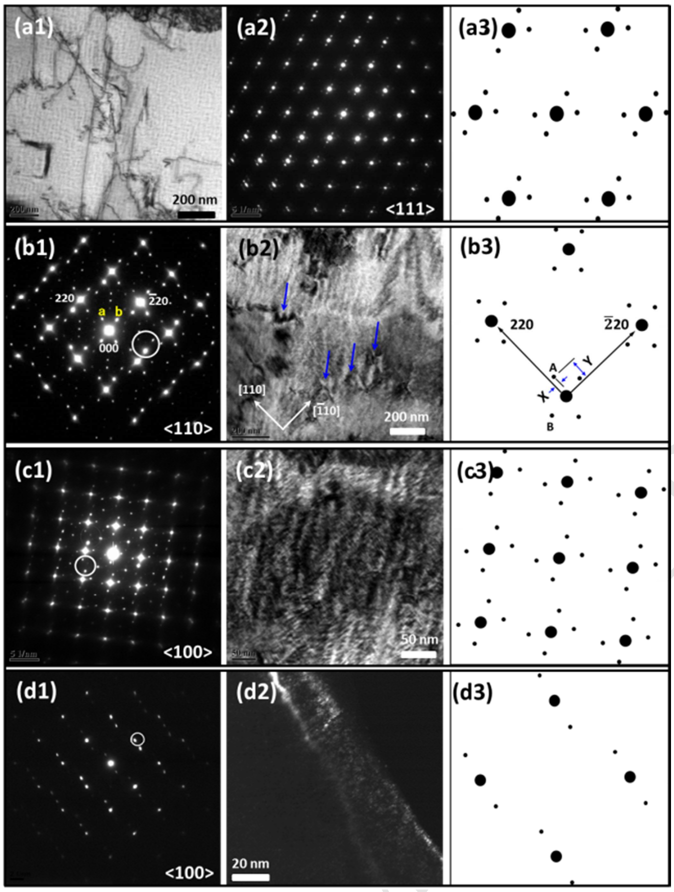

Fig.1. Bright field image of the microwire (a1) and the corresponding SAED patterns along the [111] (a2). SAED patterns along the<110> (b1), <100> (c1) and another <100> (d1) zone axis direction, and the corresponding dark field image (b2), (c2), (d2) obtained from the satellites, respectively. (a3), (b3), (c3), (d3) are the schematic diagram showing the sets of positions of the satellites observed from the corresponding SAED. (b3) illustrating four set of satellite positioned around each main diffraction spots with X fractional indices of ± 0.11 $<\bar{1}10>^{*}$ and Y fractional indices of ± 0.6 $<110>^{*}$ for the satellite.

The satellites in SAED patterns suggested that several kinds of microstructures existed in Ni_2MnGa alloys and the mystical microstructure characteristics were worth future HRTEM analysis. Fig.2 demonstrated the microstructure analysis results of the austenite of Ni-Mn-Ga microwires at RT. The fast Fourier transform (FFT) diffraction spot (a2) obtained from HRTEM image (a1) presented four satellite spots around each main spot, which is corresponding to the SAED patterns in Fig.1. The inverse fast Fourier transform (IFFT) pattern (a3) was obtained from one satellite spot in (a2), marked with number 1. The IFFT image (a3) presents the typical feature of a wave-like structure with a wave vector *V*=0.656 nm, which is close to the magnitude of that in Ni_2FeGa alloys [42]. The modulation wave vector corresponds well to the well-defined satellites. The angle between the wave vector and the atomic arrangement direction of <110> is about 14.3°. By analyzing the enlarged IFFT image (a4) of (a3), the wave vectors are found to form with periodic atomic stacking along the <110> direction. Besides, the characteristics of tweed structures are composed of 5 atomic layers according to the geometric relations. The structural fluctuation at atomic scale reveals the multiple modulations and the atomic arrangement before martensitic transformation.

Group b figures show the HRTEM image (b1) of austenite with multiple domain structure. The more complex diffraction spots (b2) indicated complex multiphase microstructure appeared in this system. Austenite was confirmed (b3) according to the IFFT image obtained from the main diffraction spot (marked with number 1) and the average interplanar spacing d of (110) plane is about 0.20 nm. Fig. 2(d) is the IFFT image of satellite spot marked with number "2" and it reveals the feature of complex domain. The modulation wave vector is calculated to be *V*=0.678 nm with periodic characteristics. The satellites are related to the tweed characteristic of austenite without changing its structure.

Moreover, multiple kinds of domain structure to coexist as shown in group c figures. The FFT spots areas marked as A and B also presents the main diffraction spots with the satellites surrounding it, as shown in Fig. 2(c1). (c2) is the IFFT image obtained from the main diffraction spot and it reveals the same structural parameter with that shown in (b3). The structures of these micromodulated domains are different, as shown in (c3) and (c4), which are obtained from the corresponding satellites from area A and B in (c1), respectively. It should be noticed that there is a different angle between the satellites and the main diffraction spots, which suggests the various micromodulated domain structure appeared in austenitic phase Ni-Mn-Ga alloys. However, the austenitic structure obtained from the main diffraction spots remains unchanged. The crossed microstructural domain structure illustrate an oblique angle of 75.6° in (c4), this kind of tilt could be result from martensitic microdomains or unmodulated premartensitic transformation in local area. The ordered micro-modulated domain structures in Fig. 2 are a kind of precursor of martensitic variants below the martensitic transformation.

Here, the satellites around the main spots reveal the “tweed structure”, i.e. micro-modulated domain structure. Single and crossed domain structures have been investigated through the TEM dark image and HRTEM imaging. The single domain with the width of tens of nanometers, as shown in Fig. 1(d2), can be obtained from one of the paired satellites. The “tweed structure” obtained from three satellites, as shown in Fig. 1(c2), represents the multiple kinds of microstructural domains. The width of the tweed structure is in the scales of tens of nanometers. During the junction place of single domain, the crossed domain structures emerge with different contrast, as marked with black arrow in Fig. 1(b2).

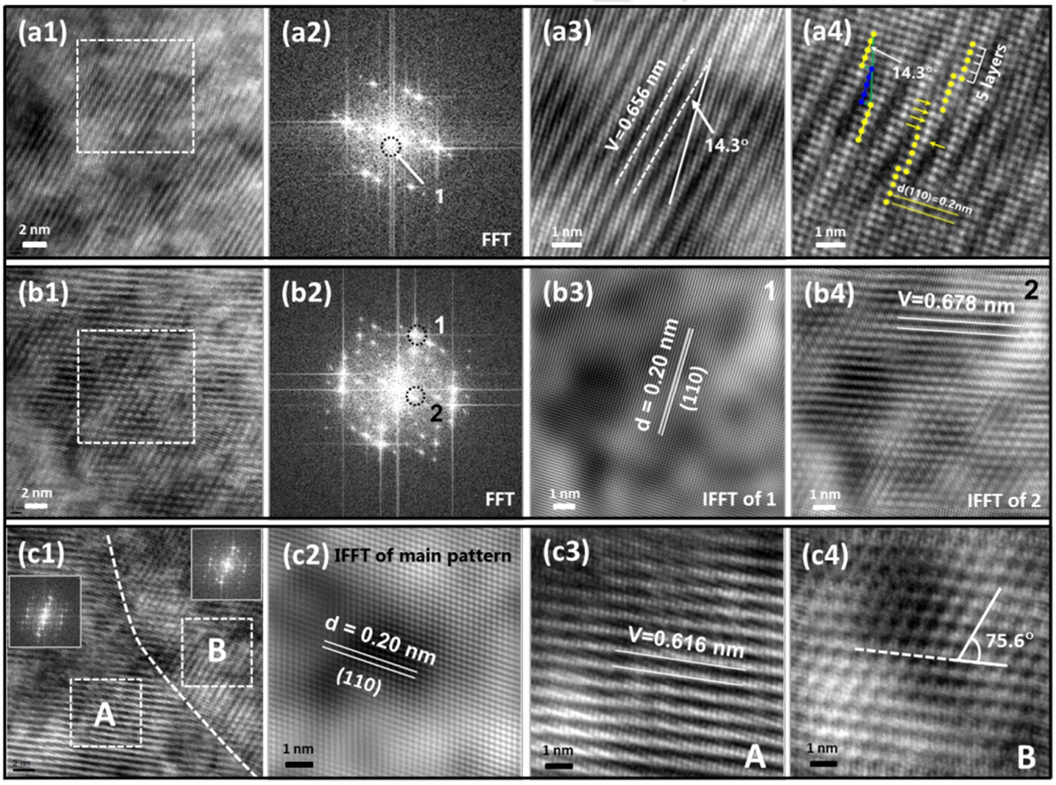

Fig.2. Microstructure analysis of the Ni-Mn-Ga microwires at RT. Group (a) figures show the single domain structure (a1) and the corresponding FFT image (a2). (a3) is the IFFT image from the satellite pattern in (a2). (a4) is the enlarged image from (a3) and it reveals the tweed structure with the periodic atomic stacking. Group (b) figures demonstrate the complex domain structure

(b1). (b3) and (b4) are the IFFT images obtained from the satellites of "1" and "2" in (b2), which is obtained by FFT in (b1). Group (c) figures show the multiple kinds of domain structure (the dotted line is the domain boundary) in (c1), and from the district A and B, the FFT images are presented. (c2) is the IFFT image obtained from the main patterns. (c3) and (c4) are the IFFT images obtained from the satellites of district A and B, and it reveals the single domain and cross domain structure respectively.

The Ni-Mn-Ga microwires are $L2_1$ cubic austenitic phase at RT and then transform into modulated martensitic variants when cooling below the martensitic transformation temperature (M_s ~264 K), as shown in Fig. 3. The constituent phase of microwires was stripe martensitic phase at 228 K and it was confirmed to be *5M* martensite according to the corresponding SAED patterns. When heating above the phase transformation temperature, the diffuse streaks disappeared and the microwires became austenite again. During this martensitic transformation, the process of PM can be confirmed; a freezing of the displacements associated with the soft phonon is generated and caused a periodic distortion and torsion of the parent cubic lattice when cooling to a certain temperature. Below the certain temperature, the PM distorts along the [110] direction due to the magnetic-elastic coupling and its relation to the lattice dynamics. A strain and commensurate shuffle lead to the quasitetragonal primitive unit cell with the c-axis parallel to any of the satellites located in equivalent position. The results suggest that the micromodulated domains are temperature dependent and are also the precursor of the martensitic transformation. Moreover, those results also verify the changes in structure and magnetic property occurring simultaneously during the martensitic transformation induced by decreasing temperature.

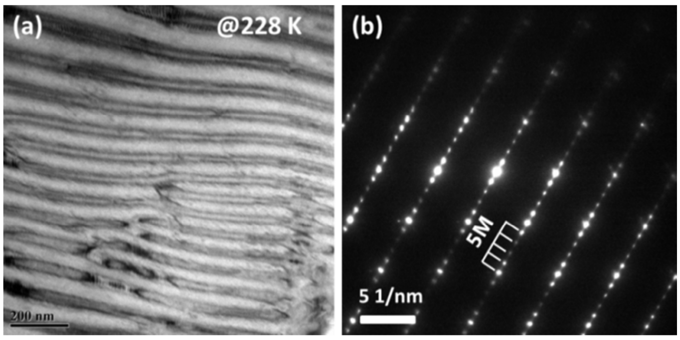

Fig.3 Bright field TEM image of Ni-Mn-Ga martensitic microwire at 228 K (a) and the

corresponding SAED confirms the *5M* modulation structure.

The model is drawn to illustrate the structural transformation of P→PM and PM→5M during cooling, as shown in Fig. 4. According to the definition of Zhang's notation [27], the stacking sequence of *5M* martensite belongs to $(3\bar{2})$ along the $[\bar{1}10]$ direction. The phase transformation process illuminated in Fig. 4(a) and (b) indicated that undergoes nonhomogeneous $\{\bar{1}10\}$<110> elastic shearing displacement. The $\{001\}_{5M}$ planes of five-layed modulated martensite are transformed from the $\{\bar{1}10\}_{cubic}$ planes of austenite when the temperature is below the M_s. The martensitic transformation temperature of $Ni_{53}Mn_{24}Ga_{23}$ microwire is between 264 K and 274 K, which is close to RT. The observation of complex microstructural domains from TEM observation at RT could be attributed to the free energy decreasing involved in localized atomic movement to form an unstable transitional state, and then it transforms to martensitic state upon subsequent cooling. The prepared shape memory microwire undergoes rapidly solidification by quenching from molten state. High solidification rate prevents the atomic ordering and makes the alloys metastable. The microdomain structure and the corresponding satellites pattern are a kind of precursor of martensitic transformation for the alloy of transitional state.

During the phase structural transformation from the $L2_1$ superstructure to *5M* modulated martensitic phase, the unit cell volume reduces by half, and the tetragonality increases and the lattice distorts with β=90.3°. Meantime, crystal structure of PM remains a complete coherence relationship with the matrix (can be seen as isostructural phase transition). But unlike the traditional martensitic transformation process, the local fluctuation of domain structure and composition emerge at this stage. The orientations of the microdomain structure are corresponding to the satellite orientations. Thus, the single domain and crossed domain structural with obvious differences can be seen during PM transformation by analyzing the satellites. The tweed contrast regions observed with periodic changes and various modulation wave vectors are the characteristics of PM Ni-Mn-Ga Heusler alloys. But this result is different from the Bain distortion of 10% Pt-substituted Ni_2MnGa alloys

[30]. Long-range ordered wave vectors have ordered structure in a single or multiple directions. The existence of the *5M*-like modulated structure in single domain structure suggests that the phase transformation process will be PM→5M. Comparing the diffraction pattern of <111> crystal zone axis between austenite and martensite, and the angular deflection between the pattern of satellites and the main diffraction spots, the phase transition process is accompanied by lattice distortion and slightly twisted. Low-symmetry martensitic phase of Ni-Mn-Ga Heusler also have tetragonal non-modulated (NM) and 7-modulated (7M) martensitic structures below M_s depending on the composition [46, 47]. A hierarchy emerged in the microstructure of Ni-Mn-Ga film exhibits the morphology martensite with micro-twins → nano-twins → modulated stacking [48]. During the martensitic transformation, the adaptive martensites can be expected under the condition that the energy of the twin boundary between the two variants is very low and elastic energy at the interface between austenite and martensite is high. Hence, the large MFIS in Ni_2MnGa with extremely low twinning stress is related to the modulated structures of premartensite and martensite phases [49]. Then the phase transformation follows to accommodate the mismatch of the crystal lattice and the martensite phase forms a coherent structure consisting of lamellae with periodic stacking of orientation variants related [46]. The modulated domain structure may also exhibit very strong coupling effect during the magnetic structural transformation from paramagnetic austenite to ferromagnetic martensite.

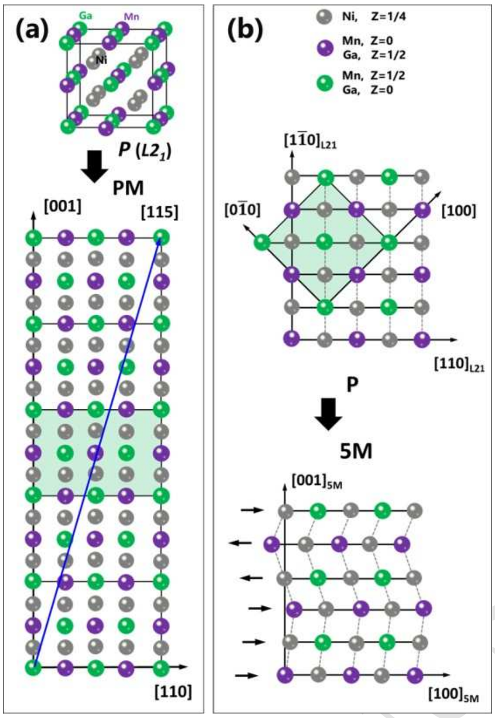

Fig. 4 Schematic model are corresponding to the structural transformation of P→PM (a) and P→5M (b) during cooling process. The wave vectors are formed with periodic lattice stacking along the [115] direction (a) and atomic projection of the (3$\bar{2}$) stacking of *5M* transformed from the L2$_1$ cubic austenitic structure (b). The arrows are the direction of the displacement of crystal planes relative to the lower plane.

4. Conclusions

The microstructural characteristics and phase transformation route of prepared Ni-Mn-Ga microwires are investigated especially the micromodulated domain characteristics by TEM and HRTEM analysis. Microstructural informtion on the single and multiple microdomains structure are obtained by analyzing the satellites surrounding the main diffraction spots. The micromodulated domain structure is aligned by atomic stacking periodically resulting in complex tweed structure, which is a kind of precursor during martensitic transformation. This phenomenon is related to the austenitic microwires prepared by rapidly solidification, which generated abundant internal stress and defects. Various domain structrues transform to five-layered modulated martensite with stripe features when the temperature is below

M_s, and the phase transformation sequence can be indicated a three step P→PM→M during cooling. The stimultaneousness of magnetic and structural transformation induced by low temperature is verified at atomic scale. This kind of complex magnetic-structural evolution can facilitate the emergence of habit plane and may exhibit better reversibility. Our findings could provide insight into the mechanism of MT and the design of advanced SMAs.

Acknowledgments

This work is supported by the National High Technology Research and Development Program of China (863 Program) under Contract No. 2015AA034101.

References

[1] S.M. Ueland, Y. Chen, C.A. Schuh, Oligocrystalline Shape Memory Alloys, Adv. Funct. Mater 22(10) (2012) 2094-2099.

[2] D.C. Dunand, P. Mullner, Size effects on magnetic actuation in Ni-Mn-Ga shape-memory alloys, Adv. Mater. 23(2) (2011) 216-32.

[3] Z. Yang, D.Y. Cong, X.M. Sun, Z.H. Nie, Y.D. Wang, Enhanced cyclability of elastocaloric effect in boron-microalloyed Ni-Mn-In magnetic shape memory alloys, Acta Mater. 127 (2017) 33-42.

[4] V.A. Chernenko, E. Villa, D. Salazar, J.M. Barandiaran, Large tensile superelasticity from intermartensitic transformations in Ni49Mn28Ga23 single crystal, Appl. Phys. Lett. 108(7) (2016) 071903.

[5] M.F. Qian, X.X. Zhang, C. Witherspoon, J.F. Sun, P. Müllner, Superelasticity and shape memory effects in polycrystalline Ni–Mn–Ga microwires, J. Alloys Compd. 577 (2013) S296-S299.

[6] M. Chmielus, X.X. Zhang, C. Witherspoon, D.C. Dunand, P. Mullner, Giant magnetic-field-induced strains in polycrystalline Ni-Mn-Ga foams, Nat Mater. 8(11) (2009) 863-6.

[7] D.Y. Cong, S. Roth, M. Pötschke, C. Hürrich, L. Schultz, Phase diagram and composition optimization for magnetic shape memory effect in Ni-Co-Mn-Sn alloys, Appl. Phys. Lett. 97(2) (2010) 021908.

[8] X.M. Sun, D.Y. Cong, K.D. Liss, Y.H. Qu, L. Ma, H.L. Suo, Y.D. Wang, Origin of anomalous cryogenic magnetic behavior in a Ni-Mn-based magnetic shape memory alloy, Appl. Phys. Lett. 110(13) (2017) 132402.

[9] A. Zhukov, V. Rodionova, M. Ilyn, A.M. Aliev, R. Varga, S. Michalik, A. Aronin, G. Abrosimova, A. Kiselev, M. Ipatov, V. Zhukova, Magnetic properties and magnetocaloric effect in Heusler-type glass-coated NiMnGa microwires, J. Alloys Compd. 575 (2013) 73-79.

[10] Z. Li, N. Xu, Y. Zhang, C. Esling, J.-M. Raulot, X. Zhao, L. Zuo, Composition-dependent ground state of martensite in Ni-Mn-Ga alloys, Acta Mater. 61(10) (2013) 3858-3865.

[11] A. Pérez-Checa, D. Musiienko, A. Saren, A. Soroka, J. Feuchtwanger, A. Sozinov, J.M. Barandiaran, K. Ullakko, V.A. Chernenko, Study of the critical parameters for magnetic field-induced strain in high temperature Ni-Mn-Ga-Co-Cu-Fe single crystals, Scripta Mater. 158

(2019) 16-19.

[12] P. Lindquist, T. Hobza, C. Patrick, P. Müllner, Efficiency of Energy Harvesting in Ni–Mn–Ga Shape Memory Alloys, Shap. Mem. Superelasticity 4(1) (2018) 93-101.

[13] J. Pons, V. Chernenko, R. Santamarta, E. Cesari, Crystal structure of martensitic phases in Ni-Mn-Ga shape memory alloys, Acta Mater. 48(12) (2000) 3027-3038.

[14] H.B. Huang, X.Q. Ma, J.J. Wang, Z.H. Liu, W.Q. He, L.Q. Chen, A phase-field model of phase transitions and domain structures of NiCoMnIn metamagnetic alloys, Acta Mater. 83 (2015) 333-340.

[15] Z.H. Nie, Y. Ren, Y.D. Wang, D.M. Liu, D.E. Brown, G. Wang, L. Zuo, Strain-induced dimensionality crossover and associated pseudoelasticity in the premartensitic phase of Ni_2MnGa, Appl. Phys. Lett. 97(17) (2010) 171905.

[16] K. Niitsu, Y. Kimura, T. Omori, R. Kainuma, Cryogenic superelasticity with large elastocaloric effect, NPG Asia Mater. 10(1) (2018) e457.

[17] S.A. Humphry-Baker, C.A. Schuh, Spontaneous solid-state foaming of nanocrystalline thermoelectric compounds at elevated temperatures, Nano Energy 36 (2017) 223-232.

[18] J.F. Wan, X.L. Lei, S.P. Chen, T.Y. Hsu, Electron–phonon coupling mechanism of premartensitic transformation in Ni_2MnGa alloy, Scripta Mater. 52(2) (2005) 123-127.

[19] H.H. Wu, A. Pramanick, Y.B. Ke, X.L. Wang, Real-space phase field investigation of evolving magnetic domains and twin structures in a ferromagnetic shape memory alloy, J. Appl. Phys. 120(18) (2016) 183904.

[20] R. Varga, T. Ryba, Z. Vargova, K. Saksl, V. Zhukova, A. Zhukov, Magnetic and structural properties of Ni-Mn-Ga Heusler-type microwires, Scripta Mater. 65(8) (2011) 703-706.

[21] J. Zhu, H. Wu, D. Wang, Y. Gao, H. Wang, Y. Hao, R. Yang, T.-Y. Zhang, Y. Wang, Crystallographic analysis and phase field simulation of transformation plasticity in a multifunctional β-Ti alloy, Int. J. Plast. 89 (2017) 110-129.

[22] S.G. Cao, Y. Li, H.H. Wu, J. Wang, B. Huang, T.Y. Zhang, Stress-Induced Cubic-to-Hexagonal Phase Transformation in Perovskite Nanothin Films, Nano Lett. 17(8) (2017) 5148-5155.

[23] C.P. Opeil, B. Mihaila, R.K. Schulze, L. Manosa, A. Planes, W.L. Hults, R.A. Fisher, P.S. Riseborough, P.B. Littlewood, J.L. Smith, J.C. Lashley, Combined experimental and theoretical investigation of the premartensitic transition in Ni2MnGa, Phys. Rev. Lett. 100(16) (2008) 165703.

[24] D.B. Gera, J. Soyama, R.D. Cava, J.E. Spinelli, C.S. Kiminami, The Influence of Sintering Parameters in the Microstructure and Mechanical Properties of a Cu-Al-Ni-Mn-Zr Shape Memory Alloy, Adv Eng Mater. 20(10) (2018) 1800372.

[25] S. Hao, L. Cui, D. Jiang, X. Han, Y. Ren, J. Jiang, Y. Liu, Z. Liu, S. Mao, Y. Wang, Y. Li, X. Ren, X. Ding, S. Wang, C. Yu, X. Shi, M. Du, F. Yang, Y. Zheng, Z. Zhang, X. Li, D.E. Brown, J. Li, A transforming metal nanocomposite with large elastic strain, low modulus, and high strength, Science 339(6124) (2013) 1191-4.

[26] H.M. Paranjape, P.P. Paul, B. Amin-Ahmadi, H. Sharma, D. Dale, J.Y.P. Ko, Y.I. Chumlyakov, L.C. Brinson, A.P. Stebner, In situ, 3D characterization of the deformation mechanics of a superelastic NiTi shape memory alloy single crystal under multiscale constraint, Acta Mater. 144 (2018) 748-757.

[27] H.R. Zhang, C. Ma, H.F. Tian, G.H. Wu, J.Q. Li, Martensitic transformation of Ni_2FeGa ferromagnetic shape-memory alloy studied via transmission electron microscopy and electron

energy-loss spectroscopy, Phys. Rev. B 77(21) (2008) 214106.
[28] F. Guillou, A.K. Pathak, D. Paudyal, Y. Mudryk, F. Wilhelm, A. Rogalev, V.K. Pecharsky, Non-hysteretic first-order phase transition with large latent heat and giant low-field magnetocaloric effect, Nat Commun. 9(1) (2018) 2925.
[29] Y. Chen, W. Xiao, K. Jiao, D. Ping, H. Xu, X. Zhao, Y. Wang, Cubic martensite in high carbon steel, Phys. Rev. Mater. 2(5) (2018) 050601.
[30] S. Singh, B. Dutta, S.W. D'Souza, M.G. Zavareh, P. Devi, A.S. Gibbs, T. Hickel, S. Chadov, C. Felser, D. Pandey, Robust Bain distortion in the premartensite phase of a platinum-substituted Ni2MnGa magnetic shape memory alloy, Nat Commun. 8(1) (2017) 1006.
[31] S. Singh, J. Bednarcik, S.R. Barman, C. Felser, D. Pandey, Premartensite to martensite transition and its implications for the origin of modulation inNi2MnGaferromagnetic shape-memory alloy, Phys. Rev. B 92(5) (2015) 054112.
[32] V. Chernenko, J. Pons, C. Seguı, E. Cesari, Premartensitic phenomena and other phase transformations in Ni-Mn-Ga alloys studied by dynamical mechanical analysis and electron diffraction, Acta Mater. 50(1) (2002) 53-60.
[33] H. Seiner, V. Kopecký, M. Landa, O. Heczko, Elasticity and magnetism of Ni2MnGa premartensitic tweed, Phys. Status Solidi B 251(10) (2014) 2097-2103.
[34] A. Sozinov, N. Lanska, A. Soroka, W. Zou, 12% magnetic field-induced strain in Ni-Mn-Ga-based non-modulated martensite, Appl. Phys. Lett. 102(2) (2013) 021902.
[35] M.F. Qian, X.X. Zhang, L.S. Wei, P.G. Martin, J.F. Sun, L. Geng, T.B. Scott, L.V. Panina, H.X. Peng, Microstructural evolution of Ni-Mn-Ga microwires during the melt-extraction process, J. Alloys Compd. 660 (2016) 244-251.
[36] P. Zheng, N.J. Kucza, C.L. Patrick, P. Müllner, D.C. Dunand, Mechanical and magnetic behavior of oligocrystalline Ni-Mn-Ga microwires, J. Alloys Compd. 624 (2015) 226-233.
[37] Z.L. Wang, P. Zheng, Z.H. Nie, Y. Ren, Y.D. Wang, P. Müllner, D.C. Dunand, Superelasticity by reversible variants reorientation in a Ni-Mn-Ga microwire with bamboo grains, Acta Mater. 99 (2015) 373-381.
[38] S.M. Ueland, C.A. Schuh, Superelasticity and fatigue in oligocrystalline shape memory alloy microwires, Acta Mater. 60(1) (2012) 282-292.
[39] Z. Ding, D. Liu, Q. Qi, J. Zhang, Y. Yao, Y. Zhang, D. Cong, J. Zhu, Multistep superelasticity of Ni-Mn-Ga and Ni-Mn-Ga-Co-Cu microwires under stress-temperature coupling, Acta Mater. 140 (2017) 326-336.
[40] Y.Y. Zhao, H. Li, H.Y. Hao, M. Li, Y. Zhang, P.K. Liaw, Microwires fabricated by glass-coated melt spinning, Rev Sci Instrum. 84(7) (2013) 075102.
[41] V. Zhukova, J.M. Blanco, P. Corte-Leon, M. Ipatov, M. Churyukanova, S. Taskaev, A. Zhukov, Grading the magnetic anisotropy and engineering the domain wall dynamics in Fe-rich microwires by stress-annealing, Acta Mater. 155 (2018) 279-285.
[42] H.R. Zhang, G.H. Wu, Atomic-size effect on the microstructural properties of Ni_2FeGa, Acta Mater. 59(3) (2011) 1249-1258.
[43] Z. Ding, J. Zhu, X. Zhang, D. Liu, Q. Qi, Y. Zhang, D. Cong, 14% recoverable strain in $Ni_{52.87}Mn_{23.82}Ga_{23.32}$ microwires, J. Phys. D. Appl. Phys. 50(9) (2017) 095303.
[44] J. Yao, X. Zheng, W. Cai, J. Sui, Effect of annealing temperature on the microstructure and mechanical properties of Ni-Mn-Ga-Gd thin film, J. Alloys Compd. 695 (2017) 1243-1247.
[45] Y. Ma, C. Jiang, Y. Li, H. Xu, C. Wang, X. Liu, Study of $Ni_{50+x}Mn_{25}Ga_{25-x}$ (x=2-11) as

high-temperature shape-memory alloys, Acta Mater. 55(5) (2007) 1533-1541.

[46] L. Zhou, M.M. Schneider, A. Giri, K. Cho, Y. Sohn, Microstructural and crystallographic characteristics of modulated martensite, non-modulated martensite, and pre-martensitic tweed austenite in Ni-Mn-Ga alloys, Acta Mater. 134 (2017) 93-103.

[47] M. Zeleny, L. Straka, A. Sozinov, O. Heczko, Transformation Paths from Cubic to Low-Symmetry Structures in Heusler Ni_2MnGa Compound, Sci Rep. 8(1) (2018) 7275.

[48] A. Sharma, S. Mohan, S. Suwas, Development of bi-axial preferred orientation in epitaxial NiMnGa thin films and its consequence on magnetic properties, Acta Mater. 113 (2016) 259-271.

[49] D. Musiienko, L. Straka, L. Klimša, A. Saren, A. Sozinov, O. Heczko, K. Ullakko, Giant magnetic-field-induced strain in Ni-Mn-Ga micropillars, Scripta Mater. 150 (2018) 173-176.

Highlights:

- Superlattice is observed in austenitic Ni-Mn-Ga microwires.
- Single and multiple microdomain structures are analyzed in premartensitic phase.
- Martensitic transformation from *P* to *5M* is confirmed by in-situ TEM observation.
- Schematic model are established to illustrate phase transformation: $P \rightarrow PM \rightarrow M$.